

# Cyber-Physical Mobility Lab: An Open-Source Platform for Networked and Autonomous Vehicles

Maximilian Kloock<sup>1</sup>, Patrick Scheffe<sup>1</sup>, Janis Maczjowski<sup>1</sup>, Alexandru Kampmann<sup>1</sup>,  
Armin Mokhtarian<sup>1</sup>, Stefan Kowalewski<sup>1</sup> and Bassam Alrifaae<sup>1</sup>

**Abstract**—This paper introduces our Cyber-Physical Mobility Lab (CPM Lab). It is an open-source development environment for networked and autonomous vehicles with focus on networked decision-making, trajectory planning, and control.

The CPM Lab hosts 20 physical model-scale vehicles ( $\mu$ Cars) which we can seamlessly extend by unlimited simulated vehicles. The code and construction plans are publicly available to enable rebuilding the CPM Lab.

Our four-layered architecture enables the seamless use of the same software in simulations and in experiments without any further adaptations. A Data Distribution Service (DDS) based middleware allows adapting the number of vehicles during experiments in a seamless manner. The middleware is also responsible for synchronizing all entities following a logical execution time approach to achieve determinism and reproducibility of experiments. This approach makes the CPM Lab a unique platform for rapid functional prototyping of networked decision-making algorithms.

The CPM Lab allows researchers as well as students from different disciplines to see their ideas developing into reality. We demonstrate its capabilities using two example experiments. We are working on a remote access to the CPM Lab via a web-interface.

## SUPPLEMENTARY MATERIAL

A demonstration video of the CPM Lab is available at <https://youtu.be/PfM0qdzorCc>.

The code, bill of materials and a construction tutorial is publicly available at <https://cpm.embedded.rwth-aachen.de>.

## I. INTRODUCTION

Testing algorithms for networked and autonomous vehicles is time-consuming and expensive. Full-scale tests of, e.g., decision-making methods require a test track. Tests on public roads may be not eligible. Nowadays, a safety driver has to be in each vehicle to monitor the movement of the vehicle and intervene if required. In addition, one vehicle is not enough to test and evaluate algorithms for networked vehicles. Therefore, multiple vehicles have to be acquired, which increases the cost and logistic overhead. Additionally, the vehicles' software have to be compatible to each other and to the infrastructure, e.g., traffic light communications. As a result, many research institutes have one full-scale test vehicle, but only a few have multiple vehicles for tests of networked algorithms.

Because of the shortcomings of full-scale experiments, simulations are the most common way to evaluate algorithms for networked vehicles. Simulations enable concepts like rapid functional prototyping, since changes in the algorithms can be rapidly applied and the results can be seen online. However, simulations abstract from real-world behavior and some aspects may not be included. This results in a big gap between simulations and real-world experiments. In order to mitigate this big gap, we developed the Cyber-Physical Mobility Lab (CPM Lab). The CPM Lab is a model-scale testing platform for networked and autonomous vehicles with focus on decision-making algorithms. The CPM Lab simulates inaccuracies due to scale absence, e.g., positioning system inaccuracies, synchronization errors, or communications problems. Hence, the CPM Lab reduces the gap between simulations and real-world full-scale experiments. Figure 1 illustrates the position of the CPM Lab in the development and testing process of networked and autonomous vehicles.

Many testbeds for model-scale autonomous vehicles exist at research institutes. They differ in many aspects, e.g., vehicle hardware, scale, cost, positioning system or communications. An overview of robots developed in the last decade that cost less than \$300 is given in [1]. All robots in this overview are with slip-stick forwards motion, e.g., [2], [3], or differential wheeled robots, e.g., [1], [4]–[12]. Labs that include vehicles with Ackermann steering geometry are presented in, e.g., [13]–[18]. When model-scale vehicles are larger, they typically carry more onboard sensors, e.g., lidar sensors and cameras, and more computation power, but are more costly and need more space to operate, e.g., [19], [20]. Communications between the vehicles include Bluetooth, radio, light signals and WLAN. Table I compares closely related labs. The comparison considers the properties: (1) Ackermann steering geometry, (2) capability for autonomous driving, (3) capability for networked driving, (4) open source availability and (5) synchronization of networked control to ensure determinism. Parentheses indicate that the property is either not the focus of the platform or that the property is given with restrictions. The widely known Duckietown [1] uses differential drive robots. Communication between the vehicles is only possible through LED signals received by an onboard camera. The F1TENTH [16] platform uses the Robot Operating System (ROS) platform for communication, so networked testing possibilities are theoretically given. It would need an extension of the architecture, as the focus of the platform lies in autonomous driving. The vehicles are twice as large as our vehicles, so the lab environment for

<sup>1</sup> Maximilian Kloock, Patrick Scheffe, Janis Maczjowski, Alexandru Kampmann, Armin Mokhtarian, Stefan Kowalewski and Bassam Alrifaae are with the Chair for Embedded Software, RWTH Aachen University, 52074 Aachen, Germany {kloock, scheffe, maczjowski, kampmann, mokhtarian, kowalewski, alrifaae}@embedded.rwth-aachen.de

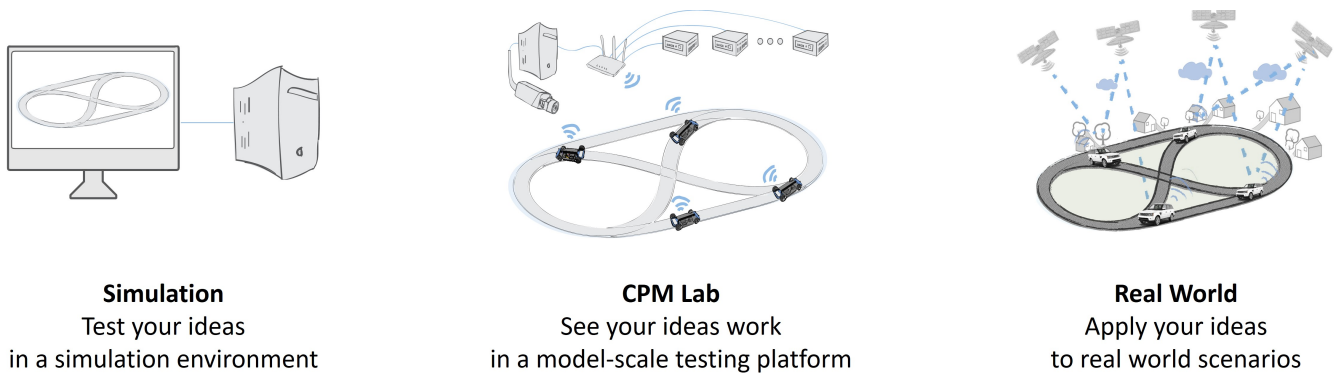


Fig. 1. An overview of the development process of simulations (left), CPM Lab experiments (middle), and real world experiments (right).

TABLE I  
RECENT GROUND VEHICLE TESTING PLATFORMS.

	Ackermann	Open source	Autonomous	Networked	Synchronous
Duckietown [1]	-	✓	✓	(✓)	-
Robotarium [12]	-	✓	✓	✓	-
F1TENTH [16]	✓	✓	✓	✓	-
Prorok Lab [17]	✓	✓	✓	✓	-
CPM Lab	✓	✓	✓	✓	✓

networked research needs to be larger as well. The characteristic feature of the Prorok Lab [17] is that all computations run on external PCs, and the vehicles only receive actuator signals via radio. The vehicles carry no onboard sensors or considerable computing power. The Robotarium [12] runs experiments with differential drive robots. It offers a remote access, so that any registered user can run experiments on swarm robotics.

The vision of our CPM Lab is to provide an open-source model-scale lab for real-time experiments and rapid-functional prototyping for networked and autonomous vehicles. Our focus is on decision-making algorithms, trajectory planning, and control. The CPM Lab simulates components for other functionalities of networked and autonomous vehicles, e.g., perception or prediction. In order to provide a testing platform that suits rapid functional prototyping approaches for networked decision-making algorithms, we also provide a simulator of the CPM Lab and all its components using the same interfaces as in the CPM Lab. This enables the seamless use of the same software in simulations and in experiments without any adaptations. The CPM Lab can test the networked system in a model-, software-, or hardware-in-the-loop scheme, referred to as X-in-the-Loop (XiL).

The remainder of this paper is structured as follows. Firstly, Section II gives a system overview of the CPM Lab containing all important modules. Section III shows the architecture and describes the interaction between all modules of the CPM Lab. Section IV presents the operation of the CPM Lab in two different scenarios. Finally, Section V

concludes the paper.

## II. LAB SETUP

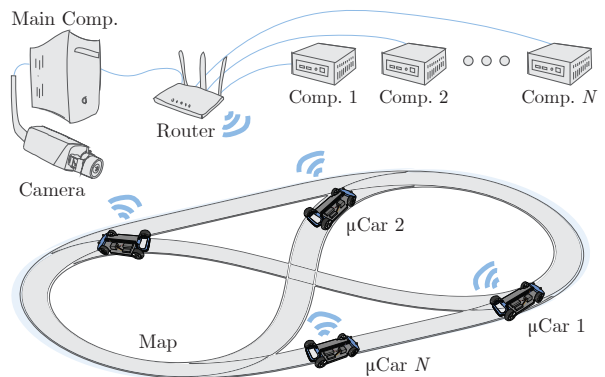


Fig. 2. An overview of the CPM Lab.

Figure 2 shows a schematic overview of the CPM Lab. It consists of

- 1) 20 model-scale vehicles ( $\mu$ Cars),
- 2) a camera for the indoor positioning system,
- 3) external computation devices,
- 4) a main computer to control and monitor experiments,
- 5) a map containing the road structure, and
- 6) a router for the communications.

The 1:18 scale  $\mu$ Cars have a length of 220 mm, a width of 107 mm, and a height of 70 mm. The maximum speed is 3.7 m/s. Figure 3 shows a picture of one  $\mu$ Car. The basis for the  $\mu$ Cars is the XRAY M18 Pro LiPo platform [21].

Figure 4 depicts the hardware architecture of the  $\mu$ Car. Each  $\mu$ Car consists of an Atmega 2560 microcontroller, a Raspberry Pi Zero W, an odometer, an IMU and a motor driver. The Atmega 2560 and the Raspberry Pi are used for computations that are described in the architecture in Section III. The odometer and IMU measure the speed, acceleration, and yaw rate. The odometer is composed of three hall-effect sensors that measure the rotation of a diametrically polarized magnet attached to the motor shaft. The motor driver controls the motor voltage through pulse width modulation. We use servos to steer the  $\mu$ Car. The 3500 mAh

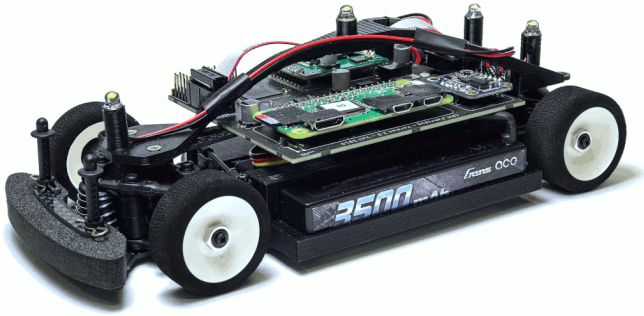


Fig. 3. A picture of a  $\mu$ Car.

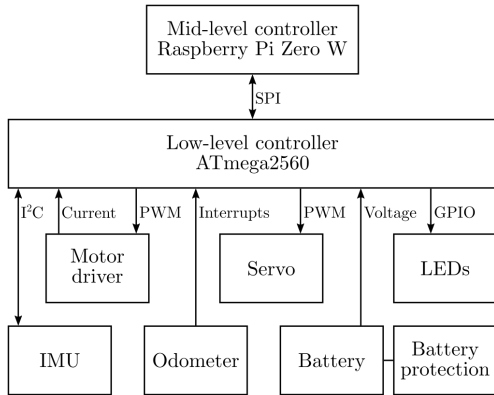


Fig. 4. Hardware architecture of the  $\mu$ Car.

batteries allow for five hour runtime. A battery protection inhibits the battery of discharging below a threshold to prevent the battery from damage. The scale of the  $\mu$ Cars approximate the scale of Volkswagen Golf 7 sized vehicles. We described in [22] the  $\mu$ Car hardware in detail.

We developed a vision-based Indoor Positioning System (IPS) that computes the positions and orientations (poses) of the  $\mu$ Cars. In order to keep the costs and computation requirements of the  $\mu$ Cars low, the poses are computed externally on the main computer. The IPS consists of a Basler acA2040 grayscale module camera that is mounted 3.3m above the track and LEDs attached to each  $\mu$ Car. Each  $\mu$ Car is equipped with four LEDs, see Figure 3. The three outer LEDs are used to determine the pose of the  $\mu$ Car. In order to map poses to  $\mu$ Cars, the IPS also identifies the  $\mu$ Cars using the fourth LED. The identification LEDs flash in unique frequencies. The IPS identifies LEDs using a 50Hz stream from the camera. We set a low exposure time to have a high contrast of the LEDs to the ambient light. By this, the LED spots are clearly identified through image processing. The three outer LEDs build a non-equilateral triangle. By this, the poses can be computed unambiguously. The poses are computed for the center of mass of the  $\mu$ Cars. Please note that the IPS provides all coordinates in a global form, i.e., the vehicles receive their coordinates in a global coordinate system. Our IPS is described in [23] in more detail.

In order to enable rapid functional prototyping, we provide external computation entities to each  $\mu$ Car. These external computation entities are Intel NUCs, equipped with i5

processors and 16 GB of RAM each. For simulation of networked computations, each  $\mu$ Car is logically connected to an Intel NUC. Each Intel NUC only performs computations for one  $\mu$ Car.

We constructed the map to fit the  $\mu$ Cars' dynamics and our space requirements. Due to the continuity of the change of the steering angle, the roadway should be two times continuous differentiable [24]. With respect to the maximum steering angle of the  $\mu$ Cars the maximum curvature of the road is limited. For space reasons, the map is limited to 4 m x 4.5 m. To keep the space requirements low, the lanes are narrow but fit to the width of the  $\mu$ Cars. The roads are for visualization only and are not detected by any mechanism of the CPM Lab. The digital representation of the map, nevertheless, is used, e.g., for decision-making.

Figure 5 shows the framework architecture of the CPM Lab. It follows the *Sense, Plan, Act* scheme, including infrastructure functionalities.

a) *Infrastructure*: The infrastructure part provides a database of scenarios, called scenario sever. Scenarios include mission plans and the simulation of non-automated traffic participants. Scenarios are defined in the Common-Road scenario format of [25]. The scenario data are stored in the map. The map is used as a database at runtime and includes static data like the road network, dynamic data like the positions of traffic participants, and preview data of planning. The road network is stored in the Lanelets road format of [26]. In order to simulate real environments, the environment model can be affected by artificial errors and noises in different intensities, e.g., to simulate positioning errors or communications delays.

b) *Sense*: Each  $\mu$ Car consists of an Inertial Measurement Unit (IMU) and an odometer. The camera externally computes the poses, i.e., positions and orientations of all  $\mu$ Cars and communicate them to all  $\mu$ Cars. This simulates GNSS. Please note that the focus of the CPM Lab is on decision-making, trajectory planning, and control. Hence, the CPM Lab simulates most of the sensors that are used in networked and autonomous vehicles.

c) *Plan*: The planning part consists of the modules coordination, decision-making, and verification. The coordination module determines the coupling of the  $\mu$ Cars for the decision-making. The decision-making consists of the submodules routing, behavior, trajectory, and control. The routing submodule plans the route from a start position to an end position. The behavior submodule plans the behavior of the  $\mu$ Car and the trajectory submodule computes trajectories. Before the trajectories are applied on the  $\mu$ Car, they are verified to ensure safety aspects, e.g., collision-freeness. Our work in [27] is an example of verification, while the works in [28]–[30] are examples of decision-making. The CPM Lab is able to execute the decision-making of multiple  $\mu$ Cars centralized, or distributed in a parallel, sequential, or hybrid manner. Section III gives more details about the decision-making architecture and Section IV presents two example experiments.

d) *Act*: The acting part consists of the decision-making submodule control and the physical actuators. The submodule control uses the planned trajectory as an input and computes corresponding control inputs, i.e., motor voltage and steering angle. The resulting commands are executed by the motor driver and servo.

### III. ARCHITECTURE

Figure 6 illustrates the architecture of the CPM Lab. It consists of High-Level Controllers (HLCs) placed on the external computation devices, a middleware, Mid-Level Controllers (MLCs) placed on the Raspberry Pis, and Low-Level Controllers (LLCs) placed on the ATmega microcontrollers. The Raspberry Pis and ATmega microcontrollers are placed on the  $\mu$ Cars. The external computation devices are logically connected to the  $\mu$ Cars. In the following, we explain all modules of the architecture in detail.

#### A. High-Level Controller (HLC)

The HLCs run on the external computation devices. They are not placed on the  $\mu$ Cars due to space and weight requirements. The HLCs are responsible for the modules coordination, decision-making and verification, see Figure 5. The HLCs send trajectories to the MLCs and receive the fused poses of the  $\mu$ Cars from the MLCs. Depending on the mode of operation, the HLC couplings are different. In the following we describe the centralized and distributed computation modes of the CPM Lab.

1) *Centralized Computation*: For centralized computation, only one HLC is needed. This HLC is logically connected to all  $\mu$ Cars and plans trajectories depending on all  $\mu$ Car states, objectives, and constraints. The output of the central HLC consists of one trajectory for each vehicle. Figure 7(a) depicts the architecture for centralized planning.

2) *Distributed Computation*: In distributed computation mode, each vehicle is logically connected to an unique HLC, i.e., there is a one-to-one mapping for HLC to vehicle. This mode represents a system in which each  $\mu$ Car on the road plans its own trajectory without a central coordinator. The trajectory planning requires some cooperation between the HLCs. Figure 7(b) depicts the architecture for distributed planning.

#### B. Middleware

The middleware runs on the external computation devices and on the Raspberry Pis on the  $\mu$ Cars. It synchronizes the computations of the HLCs and the MLCs using the concepts of the logical execution time approach [31].

The middleware is based on the Data Distribution Service (DDS), which is a standardized protocol for decentralized communications in distributed systems based on the publish-subscribe pattern [32]. Besides being used in safety-critical systems, such as medical devices and air traffic control [33], DDS is also entering the automotive domain as part of the upcoming AUTOSAR Adaptive platform [34]. The protocol offers a variety of configurable Quality-of-Service (QoS) parameters, including dependable or best-effort communications. In contrast to the widespread ROS [35], DDS does

not rely on a designated entity for service discovery or binding, which makes the resulting architecture more robust. However, in contrast to DDS ROS comes along with many packages and tools to support the development process.

At its core, DDS uses the User Datagram Protocol (UDP), which leads to lower communications latencies than middlewares based on the Transmission Control Protocol (TCP), such as ROS or Message Queuing Telemetry Transport (MQTT) [36]. This is because UDP does not require an acknowledgment for each packet. We do not rely on retransmitting the dropped packets, because the data is time-critical and become obsolete when a packet is dropped. Through the use of DDS, a variable number of  $\mu$ Cars can be part of experiments, without having to adapt the underlying communications architecture. Additionally, the CPM Lab architecture becomes more adaptable for extensions through the dynamic coupling of components in the communications architecture. Various commercial and open source implementations of DDS are available <sup>1,2</sup>. We use the RTI Connex DDS implementation<sup>3</sup>.

#### C. Mid-Level Controller (MLC)

The MLCs run on Raspberry Pis which are mounted on the  $\mu$ Cars. The MLCs provide two modes of operation: direct control and trajectory following. In direct control, the MLCs receive commands of torque and steering angle from the HLCs. In trajectory following, the MLCs receive trajectory nodes of the form  $[t_i, x_i, y_i, v_{x,i}, v_{y,i}]$ , where  $t_i \in \mathbb{R}^+$  represents the time at which  $\mu$ Car  $i \in \mathbb{N}$  should be at position  $[x_i, y_i] \in \mathbb{R} \times \mathbb{R}$  with velocity  $[v_{x,i}, v_{y,i}] \in \mathbb{R} \times \mathbb{R}$  in  $x$  and  $y$  direction, respectively. The continuous reference trajectory  $[x_{ref}(t), y_{ref}(t)]$  is constructed using Cubic Hermite spline interpolation, which interpolates between the trajectory nodes. The use of Hermite interpolation allows the addition of trajectory nodes in real time without affecting the interpolation between previous nodes. The MLCs implement trajectory following controllers based on Model Predictive Control (MPC). The MLCs perform sensor fusions and use the fused poses of the on-board odometers and IMUs and from the IPS via wireless communications. The computed torques and steering angles are communicated to the LLCs.

#### D. Low-Level Controller (LLC)

The LLCs run on ATmega 2560 microcontrollers on the  $\mu$ Cars. They act as a hardware abstraction layer and sample the on-board sensors, convert the sensor signals into data compatible to the MLCs, and send the sensor data to the MLCs. The LLCs apply the torque and steering angle given by the MLCs to the actuators and convert the control inputs into signals compatible with the  $\mu$ Cars' hardware.

## IV. EXPERIMENTS

We present the use cases of the CPM Lab in multiple example experiments. The experiments are implemented in

<sup>1</sup><http://www.eprosima.com>

<sup>2</sup><http://www.opendds.org>

<sup>3</sup><https://www.rti.com/products/dds-standard>

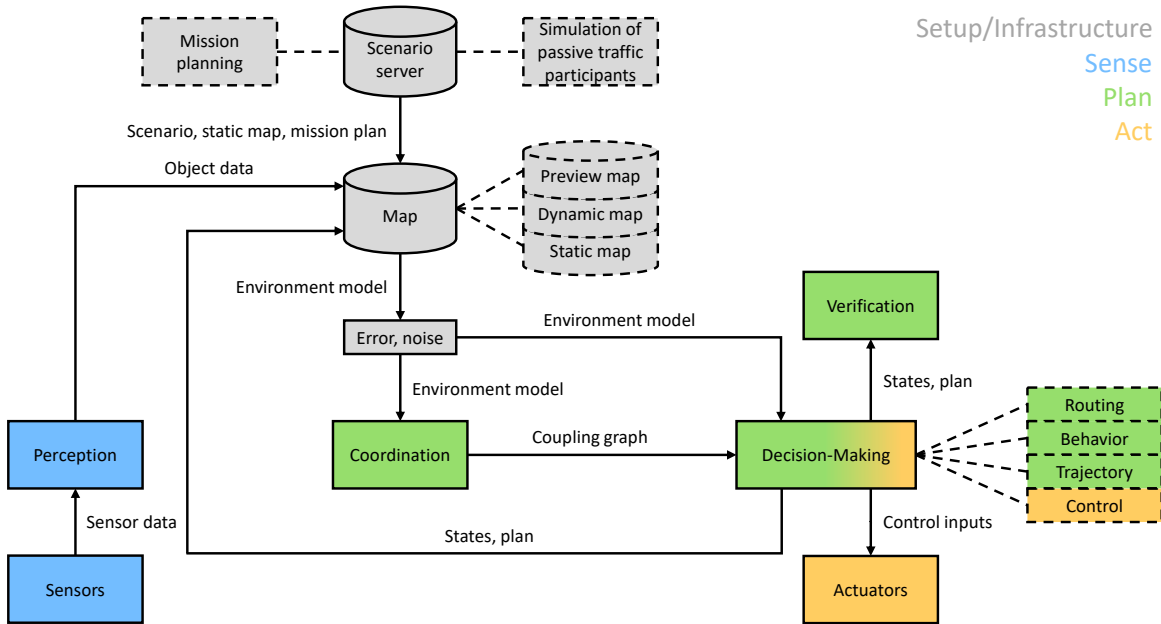


Fig. 5. Framework concept. Colors illustrate the logical affiliation. Grey, blue, green and yellow denote infrastructure, *Sense*, *Plan* and *Act*, respectively.

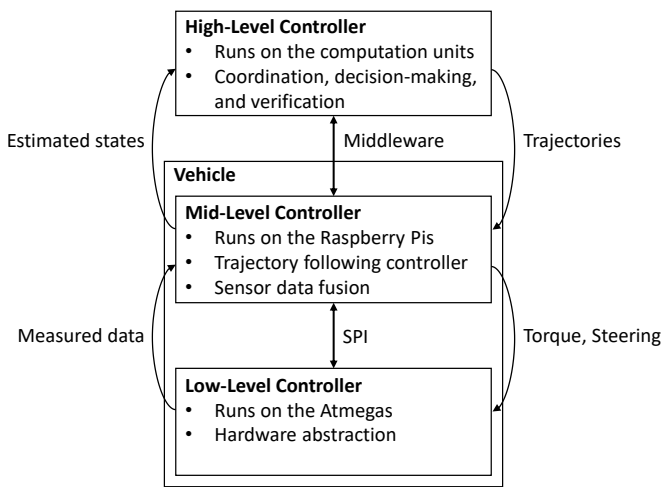
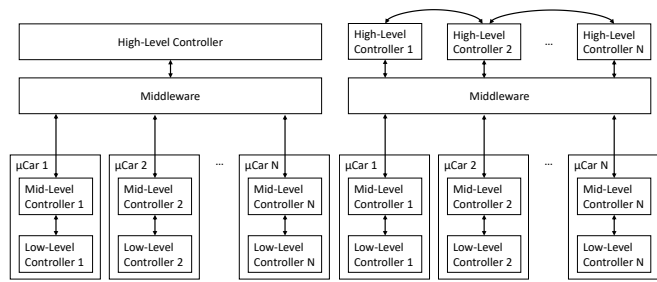


Fig. 6. The architecture of the CPM Lab is divided into HLC, middleware, MLC, and LLC. The architecture is placed on external computation devices, Raspberry Pis, and ATmega microcontrollers.



(a) Architecture of centralized planning. (b) Architecture of distributed planning.

Fig. 7. The architectures for centralized and distributed planning. In centralized planning, there is only one HLC for all  $\mu$ Cars.

different programming languages. First, we show one experiment with different amount of  $\mu$ Cars and different mixtures of real and simulated  $\mu$ Cars. Afterwards, we evaluate the distributed planning in the CPM Lab. Videos of the presented experiments are shown in the demonstration video available on <https://youtu.be/JWOyf19-nKg>.

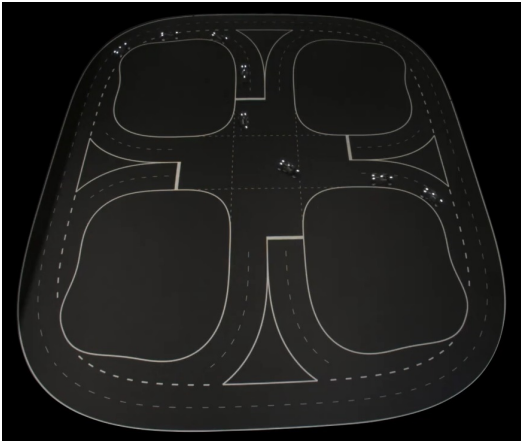
#### A. Real and Simulated $\mu$ Cars

For the evaluation of real and simulated  $\mu$ Cars, we start with a platoon scenario. The platoon scenario consists of a leader  $\mu$ Car and an arbitrary number of following  $\mu$ Cars. The leading  $\mu$ Car plans its trajectory given the path and a reference speed. The following  $\mu$ Cars adapt the trajectory used by the leading  $\mu$ Car in order to follow it. This experiment is implemented in MATLAB. Figure 8 shows eight  $\mu$ Cars on the test track in the CPM Lab. Figure 8(a) shows the view on the physical test track and Figure 8(b) shows the visualization.

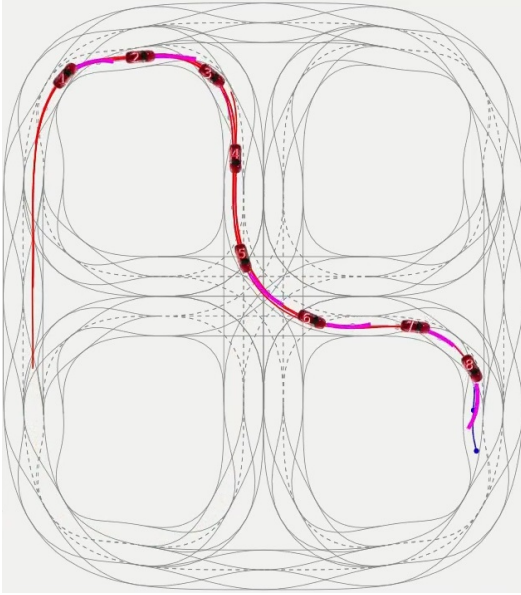
We replaced two real  $\mu$ Cars with two simulated  $\mu$ Cars and evaluated the platoon scenario again. Figure 9 shows the test track in the CPM Lab. Figure 9(a) shows the physical track with 6 real  $\mu$ Cars and Figure 9(b) shows the visualization. The visualization also shows the simulated  $\mu$ Cars, since the CPM Lab does not differ between those. Therefore, the real  $\mu$ Cars behave as if all  $\mu$ Cars were driving on the physical track. No modifications of the source code are required, even for using only simulated  $\mu$ Cars. Therefore, the implementation for decision-making can be developed in simulations without the need for any additional hardware than the main computer, see Section II. The task of the main computer can be done by any desktop or laptop computer.

#### B. Distributed Computations

For the evaluation of distributed computations in the CPM Lab, we used an intersection scenario. In the inter-



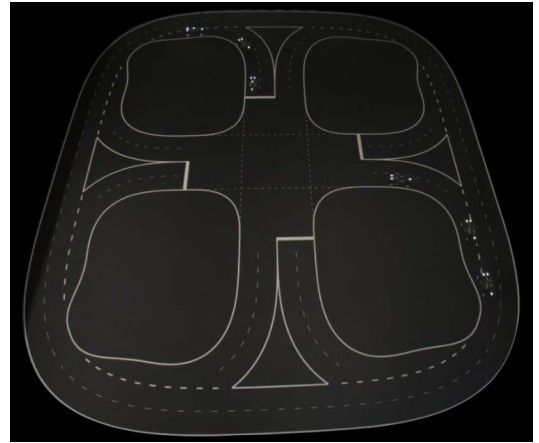
(a) Physical test track in the CPM Lab.



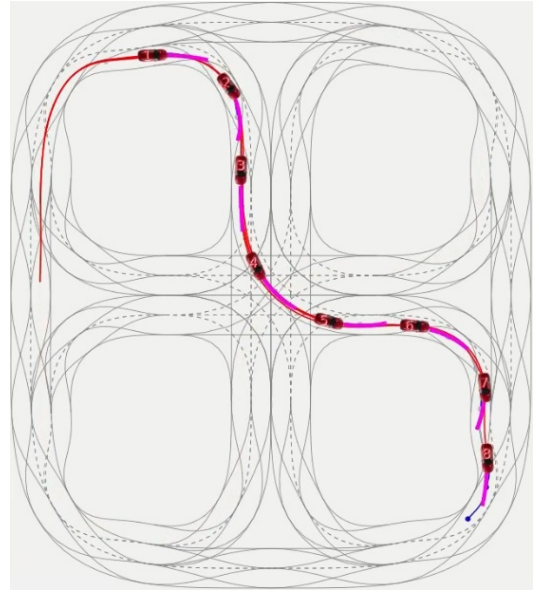
(b) Visualization of the test track.

Fig. 8. The test track of the CPM Lab with a platoon consisting of 8  $\mu$ Cars. The blue lines represent the  $\mu$ Cars' prediction horizon in the HLCs, the purple lines represent the control horizon in the MLCs, and the red lines represent the driven path of the  $\mu$ Cars.

section scenario,  $\mu$ Cars plan their trajectories on the path given a reference speed. The path is chosen randomly at each junction in order to balance left and right moves of the  $\mu$ Cars and to simulate real traffic. Then,  $\mu$ Cars avoid collisions using a priority-based scheme as proposed in [37]. We statically prioritized the  $\mu$ Cars by defining unique  $\mu$ Car IDs. The lower the ID of a  $\mu$ Car the more important it is in the trajectory planning.  $\mu$ Cars ignore collisions with  $\mu$ Cars of higher ID. Therefore, the responsibility of collision avoidance is at  $\mu$ Cars with higher IDs.  $\mu$ Cars with higher IDs reduce their speed to avoid collisions with  $\mu$ Cars with lower IDs. After avoiding a collision, the  $\mu$ Cars accelerate to their reference speed. Please note that in this scenario  $\mu$ Cars avoid collisions by speed reduction only. The path is not adapted for collision avoidance. This experiment is implemented in



(a) Physical test track in the CPM Lab.



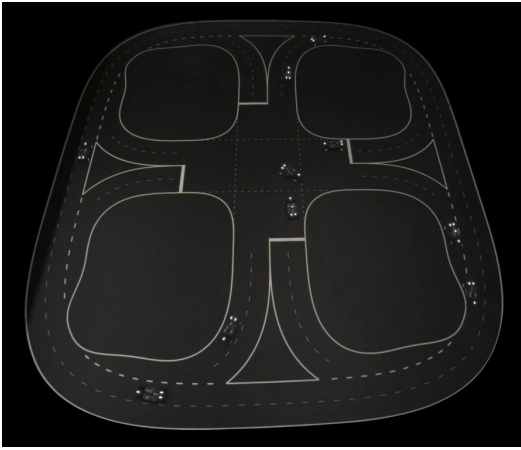
(b) Visualization of the test track.

Fig. 9. The test track of the CPM Lab with a platoon consisting of 6 real  $\mu$ Cars and 2 simulated  $\mu$ Cars. The blue lines represent the  $\mu$ Cars' prediction horizon in the HLCs, the purple lines represent the control horizon in the MLCs, and the red lines represent the driven path of the  $\mu$ Cars.

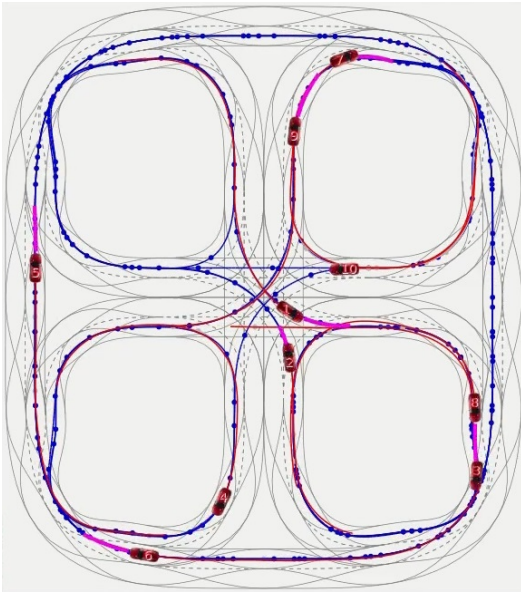
C++. Figure 10 shows the test track of the CPM Lab with 8  $\mu$ Cars in the intersection scenario.

### C. Infrastructure Stress-Test

For testing our infrastructure, including the WiFi communications between the HLCs and  $\mu$ Cars at high load, we placed 18  $\mu$ Cars on the map and let them drive on the outer circle with a fixed speed. Therefore, no collision avoidance is required. The HLC sent trajectories for the  $\mu$ Cars in a frequency of 100 ms. Figure 11(a) shows the real test track of the CPM Lab and Figure 11(b) shows the visualization. The infrastructure of the CPM Lab is able to handle 18  $\mu$ Cars on the track with still enough resources to perform tasks in real time. Please note that this infrastructure test only evaluates the CPM Lab infrastructure and not a specific decision-making algorithm, since the decision-making is static in this



(a) Physical test track in the CPM Lab.



(b) Visualization of the test track.

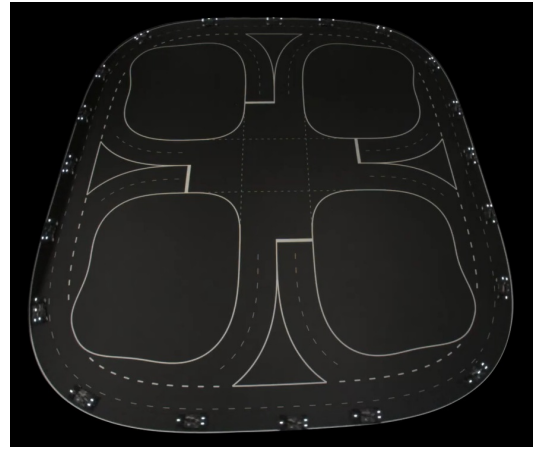
Fig. 10. The test track of the CPM Lab with 8  $\mu$ Cars driving in our intersection example. The blue lines represent the  $\mu$ Cars' prediction horizon in the HLCs, the purple lines represent the control horizon in the MLCs, and the red lines represent the driven path of the  $\mu$ Cars.

test. The purpose is to evaluate the CPM Lab at its limits of 18  $\mu$ Cars. Currently, we are assembling 2 more  $\mu$ Cars to complete the fleet of 20  $\mu$ Cars.

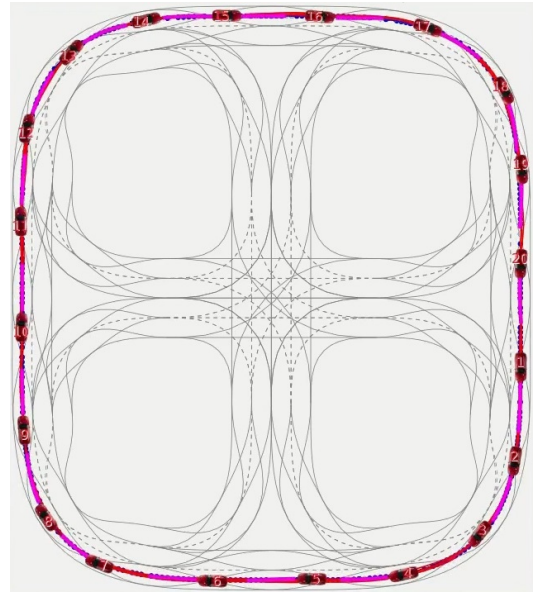
## V. CONCLUSION

This paper presented the CPM Lab, a seamless development environment for networked and autonomous vehicles with focus on decision-making, trajectory planning, and control. We presented two example experiments in our CPM Lab. The experiments differ in their programming language and computation architecture.

Furthermore, we presented our four-layered architecture that enables the use of the same software in simulations and experiments without any adaptations. Our middleware allows to adapt the number of vehicles during experiments and simulations. The CPM Lab can extend experiments with the



(a) Physical test track in the CPM Lab.



(b) Visualization of the test track.

Fig. 11. The test track of the CPM Lab with 18  $\mu$ Cars driving in our circle example. The blue lines represent the  $\mu$ Cars' prediction horizon in the HLCs, the purple lines represent the control horizon in the MLCs, and the red lines represent the driven path of the  $\mu$ Cars.

20 model-scale vehicles by unlimited additional simulated vehicles. We developed an architecture of HLC, MLC, LLC, and middleware to apply new trajectories in the vehicles deterministically and synchronously in a logical execution time approach. Furthermore, we developed the vehicles based on a model-scale RC platform and an IPS that computes the poses of the vehicles on the map. We used the CPM Lab in two practical courses in different study programs with 30 students each.

### A. Outlook

We are developing a remote-access to the CPM Lab. This will allow researchers and students to use the CPM Lab without personal presence. For more convenient experiments, we will implement our method from [38] in the CPM Lab to automatically drive the vehicles to their starting poses

of experiments. Furthermore, we will apply methods of our previous and future research in the CPM Lab.

## ACKNOWLEDGMENT

This research is supported by the Deutsche Forschungsgemeinschaft (DFG, German Research Foundation) within the Priority Program SPP 1835 “Cooperative Interacting Automobiles” and the Post Graduate Program GRK 1856 “Integrated Energy Supply Modules for Roadbound E-Mobility”.

## REFERENCES

- [1] L. Paull, J. Tani, H. Ahn, J. Alonso-Mora, L. Carlone, M. Cap, Y. F. Chen, C. Choi, J. Dusek, Y. Fang *et al.*, “Duckietown: an open, inexpensive and flexible platform for autonomy education and research,” in *2017 IEEE International Conference on Robotics and Automation (ICRA)*. IEEE, 2017, pp. 1497–1504.
- [2] M. Rubenstein, C. Ahler, and R. Nagpal, “Kilobot: A low cost scalable robot system for collective behaviors,” in *2012 IEEE International Conference on Robotics and Automation*. IEEE, 2012, pp. 3293–3298.
- [3] M. Rubenstein, B. Cimino, R. Nagpal, and J. Werfel, “Aerobot: An affordable one-robot-per-student system for early robotics education,” in *2015 IEEE International Conference on Robotics and Automation (ICRA)*. IEEE, 2015, pp. 6107–6113.
- [4] P. Robinette, R. Meuth, R. Dolan, D. Wunsch, R. E. Solutions, LLC, Rolla, and M. USA, “Labrat: Miniature robot for students, researchers, and hobbyists,” in *The 2009 IEEE/RSJ International Conference on Intelligent Robots and Systems October 11-15, 2009 St. Louis, USA*. IEEE, 2009.
- [5] S. Kernbach, “Swarmrobot.org – open-hardware microbot project for large-scale artificial swarms,” *arXiv preprint arXiv:1110.5762*, 2011.
- [6] R. K. Cole, “Stem outreach with the boe-bot,” in *Robots in K-12 Education: A New Technology for Learning*. IGI Global, 2012, pp. 245–265.
- [7] F. Riedo, M. Chevalier, S. Magnenat, and F. Mondada, “Thymio ii, a robot that grows wiser with children,” in *2013 IEEE Workshop on Advanced Robotics and its Social Impacts*. IEEE, 2013, pp. 187–193.
- [8] J. McLurkin, A. McMullen, N. Robbins, G. Habibi, A. Becker, A. Chou, H. Li, M. John, N. Okeke, J. Rykowski *et al.*, “A robot system design for low-cost multi-robot manipulation,” in *2014 IEEE/RSJ international conference on intelligent robots and systems*. IEEE, 2014, pp. 912–918.
- [9] S. Wilson, R. Gameraos, M. Sheely, M. Lin, K. Dover, R. Gevorkyan, M. Haberland, A. Bertozzi, and S. Berman, “Pheeno, a versatile swarm robotic research and education platform,” *IEEE Robotics and Automation Letters*, vol. 1, no. 2, pp. 884–891, 2016.
- [10] A. Stager, L. Bhan, A. Malikopoulos, and L. Zhao, “A scaled smart city for experimental validation of connected and automated vehicles,” *arXiv preprint arXiv:1710.11408*, 2017.
- [11] C. Márquez-Sánchez, M. Antonio-Cruz, J. Sandoval-Gutiérrez, V. E. Quiroz-Velázquez, and C. A. Merlo-Zapata, “Construction of a Low-cost Wheeled Mobile Robot for Testing Automatic Control Techniques,” in *2019 International Conference on Mechatronics, Electronics and Automotive Engineering (ICMEAE)*. IEEE, 2019, pp. 102–107.
- [12] D. Pickem, P. Glotfelter, L. Wang, M. Mote, A. Ames, E. Feron, and M. Egerstedt, “The robotarium: A remotely accessible swarm robotics research testbed,” in *2017 IEEE International Conference on Robotics and Automation (ICRA)*. IEEE, 2017, pp. 1699–1706.
- [13] A. Liniger, A. Domahidi, and M. Morari, “Optimization-based autonomous racing of 1:43 scale RC cars,” *Optimal Control Applications and Methods*, jul 2014.
- [14] J. Gonzales, F. Zhang, K. Li, and F. Borrelli, “Autonomous drifting with onboard sensors,” in *Proceedings of the 13th International Symposium on Advanced Vehicle Control (AVEC)*, 2016.
- [15] S. Karaman, A. Anders, M. Boulet, J. Connor, K. Gregson, W. Guerra, O. Guldner, M. Mohamoud, B. Plancher, R. Shin *et al.*, “Project-based, collaborative, algorithmic robotics for high school students: Programming self-driving race cars at mit,” in *Integrated STEM Education Conference (ISEC)*. IEEE, 2017.
- [16] M. O’Kelly, V. Sukhil, H. Abbas, J. Harkins, C. Kao, Y. Vardhan Pant, R. Mangharam, D. Agarwal, M. Behl, P. Burgio, and M. Bertogna, “F1/10: An Open-Source Autonomous Cyber-Physical Platform,” *arXiv e-prints*, p. arXiv:1901.08567, Jan 2019.
- [17] N. Hyldmar, Y. He, and A. Prorok, “A Fleet of Miniature Cars for Experiments in Cooperative Driving,” *arXiv e-prints*, p. arXiv:1902.06133, Feb 2019.
- [18] A. Bemani and N. Bjorsell, “Cyber-Physical Control of Indoor Multi-vehicle Testbed for Cooperative Driving,” *arXiv preprint arXiv:2006.04421*, 2020.
- [19] M. Reiter, M. Wehr, F. Sehr, A. Trzuskowsky, R. Taborsky, and D. Abel, “The IRT-buggy – vehicle platform for research and education,” *IFAC-PapersOnLine*, jul 2017.
- [20] B. Vedder, J. Vinter, and M. Jonsson, “A low-cost model vehicle testbed with accurate positioning for autonomous driving,” *Journal of Robotics*, vol. 2018, 2018, publisher: Hindawi.
- [21] XRAY, “M18 PRO LiPo,” Website, 12 2010, viewed 31 October 2019. [Online]. Available: [https://www.teamxray.com/teamxray/products/proddesc.php?prod\\_id=3622&kategoria=0&catName=XRAY%20M18%20PRO%20LiPo](https://www.teamxray.com/teamxray/products/proddesc.php?prod_id=3622&kategoria=0&catName=XRAY%20M18%20PRO%20LiPo)
- [22] P. Scheffe, M. Kloock, A. Derks, J. Maczjowski, B. Alrifaae, and S. Kowalewski, “Networked and autonomous model-scale vehicles for experiments in research and education,” 2020, IFAC World Congress, accepted.
- [23] M. Kloock, P. Scheffe, I. Tülleners, J. Maczjowski, B. Alrifaae, and S. Kowalewski, “Vision-based real-time indoor positioning system for multiple vehicles,” *arXiv preprint arXiv:2002.05755*, 2020.
- [24] D. Meek and D. Walton, “Clothoid spline transition spirals,” *Mathematics of computation*, vol. 59, no. 199, pp. 117–133, 1992.
- [25] M. Althoff, M. Koschi, and S. Manzing, “CommonRoad: Composable benchmarks for motion planning on roads,” in *2017 IEEE Intelligent Vehicles Symposium (IV)*. IEEE, 2017, pp. 719–726.
- [26] P. Bender, J. Ziegler, and C. Stiller, “Lanelets: Efficient map representation for autonomous driving,” in *2014 IEEE Intelligent Vehicles Symposium Proceedings*. IEEE, 2014, pp. 420–425.
- [27] M. Völker, M. Kloock, L. Rabanus, B. Alrifaae, and S. Kowalewski, “Verification of cooperative vehicle behavior using temporal logic,” *IFAC-PapersOnLine*, vol. 52, no. 8, pp. 99–104, 2019.
- [28] B. Alrifaae, F.-J. Heßeler, and D. Abel, “Coordinated non-cooperative distributed model predictive control for decoupled systems using graphs,” *IFAC-PapersOnLine*, vol. 49, no. 22, pp. 216–221, 2016.
- [29] M. Kloock, P. Scheffe, S. Marquardt, J. Maczjowski, B. Alrifaae, and S. Kowalewski, “Distributed model predictive intersection control of multiple vehicles,” in *2019 IEEE Intelligent Transportation Systems Conference (ITSC)*. IEEE, 2019, pp. 1735–1740.
- [30] M. Kloock, P. Scheffe, L. Botz, J. Maczjowski, B. Alrifaae, and S. Kowalewski, “Networked model predictive vehicle race control,” in *2019 IEEE Intelligent Transportation Systems Conference (ITSC)*. IEEE, 2019, pp. 1552–1557.
- [31] T. A. Henzinger, B. Horowitz, and C. M. Kirsch, “Giotto: A time-triggered language for embedded programming,” in *International Workshop on Embedded Software*. Springer, 2001, pp. 166–184.
- [32] G. Pardo-Castellote, “OMG data-distribution service: Architectural overview,” in *23rd International Conference on Distributed Computing Systems Workshops, 2003. Proceedings*. IEEE, 2003, pp. 200–206.
- [33] Object Management Group, “Who’s Using DDS?” <https://www.omgwiki.org/dds/who-is-using-dds-2/>, 2019, [Online].
- [34] S. Fürst and M. Bechter, “Autosar for connected and autonomous vehicles: The autosar adaptive platform,” in *2016 46th annual IEEE/IFIP international conference on Dependable Systems and Networks Workshop (DSN-W)*. IEEE, 2016, pp. 215–217.
- [35] M. Quigley, K. Conley, B. Gerkey, J. Faust, T. Foote, J. Leibs, R. Wheeler, and A. Y. Ng, “ROS: an open-source Robot Operating System,” in *ICRA workshop on open source software*, vol. 3, no. 3.2. Kobe, Japan, 2009, p. 5.
- [36] I. B. M. C. (IBM) and Eurotech, *MQTT V3.1 Protocol Specification*, 2010.
- [37] B. Alrifaae, “Networked model predictive control for vehicle collision avoidance: Vernetzte modellbasierte prädiiktive regelung zur kollisionsvermeidung von fahrzeugen,” Ph.D. dissertation, RWTH Aachen University, 2017.
- [38] M. Kloock, L. Kragl, J. Maczjowski, B. Alrifaae, and S. Kowalewski, “Distributed model predictive pose control of multiple nonholonomic vehicles,” in *2019 IEEE Intelligent Vehicles Symposium (IV)*. IEEE, 2019, pp. 1620–1625.